UNCLASSIFIED

AD $\underline{426763}$

DEFENSE DOCUMENTATION CENTER

FOR

SCIENTIFIC AND TECHNICAL INFORMATION

CAMERON STATION, ALEXANDRIA, VIRGINIA

UNCLASSIFIED

HYDRA PROGRAM - THEORETICAL AND
EXPERIMENTAL DETERMINATION OF
ENERGY PARTITION OF
SELECTED UNDERWATER EXPLOSIVES

by
M. Kaltwasser

JAN 20 1964

U.S. NAVAL RADIOLOGICAL DEFENSE LABORATORY

SAN FRANCISCO · CALIFORNIA · 94135

RADIOLOGICAL EFFECTS BRANCH
E.A. Schuert, Head
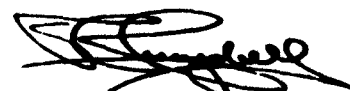
CHEMICAL TECHNOLOGY DIVISION
L.H. Gevantman, Head

ADMINISTRATIVE INFORMATION

AVAILABILITY OF COPIES

Eugene P. Cooper
Scientific Director

D.C. Campbell, CAPT USN
Commanding Officer and Director

ABSTRACT

A summary is presented of the derivation of the equation of motion
of the bubble due to an underwater spherical explosion. Migration and
surface effects are included. The formulae for the first maximum radius
and the first oscillation period, including surface effects, are given.

From the experimentally determined bubble period data and the
theoretical period formula:

$$T_2 = KW^{1/3}Z^{-5/6}\left[1.0 + KW^{1/3}Z^{-1/3}HF/(D+B)\right]$$

the energy partitions of three explosives, Pentolite, RDX + Alum (50/50),
and $2H_2 + O_2$ are calculated.

1

SUMMARY

The Problem

To compare underwater explosions producing steam bubbles and non-condensable gas bubbles on the basis of their computed energy partition values. To determine which of three selected chemical explosives best simulate an underwater nuclear explosion.

Findings

Using Friedman's formula for the bubble oscillation period and the experimentally determined bubble periods from Hydra studies, the energy partition values (i.e., fraction of charge energy left for bubble oscillation after shock passage) of three explosives were found to be:

Explosive	r
Pentolite	0.45 ± 0.12
RDX + Alum	0.50 ± 0.14
$2H_2 + O_2$	0.41 ± 0.11

Since the minimum error variation in energy partition is much greater than the variation due to type of explosive, it makes little difference which explosive (steam or non-condensable gas) is selected to simulate the nuclear case.

CONTENTS

INTRODUCTION

Underwater nuclear explosions form steam bubbles whose dynamics determine the early dispersion of the radioactivity produced. To simulate nuclear explosions, the Hydra program had been using chemical high explosives (e.g. Pentolite) which form non-condensable gas bubbles. In an attempt to more accurately simulate these detonations, two steam producing explosives were developed: an equal mixture by weight of RDX + Alum (i.e., $AlNH_4(SO_4)_2 \cdot 12H_2O$), and a pressurized stoichiometric mixture of hydrogen and oxygen. Using these two explosives and Pentolite, a series of experiments was undertaken during the summer of 1960 to determine the variation of bubble parameters between chemical explosives producing condensable steam bubbles and non-condensable gas bubbles.

The bubble parameter usually compared is the energy partition value (i.e., the fraction of charge energy left for bubble oscillation after shock passage). This is best determined from the theoretical formula for the bubble oscillation period using experimental data.

This report reviews the bubble dynamics theory that has been developed over the past several decades including surface effects. Using these theories and the bubble period data from Hydra studies, the energy partition values for selected explosives of interest have been determined.

In the literature, the first order approximation, relating the bubble period constant K to the cube root of the bubble energy is well known. However, the second order effects of fixed and free surfaces on the bubble period are generally ignored. Where these effects are

1

mentioned, the approaches are difficult to follow because of inconsist-
encies or incompleteness. After a critical review of the literature,
Friedman's papers were found to be the first and only rigorous qualitative
and quantitative determination of surface effects.

Because no papers were found to use Friedman's method to its full
advantage, and because Friedman's original work is more detailed than
necessary for the field engineer, the following section on bubble
dynamics was undertaken with effort to present a comprehensive and co-
herent outline of the equations of motion using a consistent system of
symbols in a concise package permitting bubble period prediction.

SECTION 1

DYNAMICS

1.1 EQUATION OF MOTION

The earliest derivation of the equation of motion of the gas bubble is that of Ramsauer.[1] He used the energy balance:

$$E_o = E + WD + KE \qquad (1.1)$$

which translated to words says that the initial internal bubble energy E_o, equals the internal energy at a later time E, plus the work of displacement against the water WD, plus the kinetic energy imparted to the surrounding water at any later time KE. Here

$$E_o = P_o V_o / (\gamma - 1)$$

$$E = PV / (\gamma - 1)$$

$$WD = P_h (V - V_o)$$

$$KE = 2\pi \rho A^3 \dot{A}^2$$

Assuming the bubble expands adiabatically, then

$$PV^\gamma = P_o V_o^{\ \gamma} \qquad (1.2)$$

Note: See Appendix 7 for definition of symbols.

3

and Eq. 1.1 can be rewritten as

$$P_o/(\gamma-1)\left[(A_o/A)^3 - (A_o/A)^{3\gamma}\right] + P_h\left[(A_o/A)^3 - 1\right] = 3\rho\dot{A}^2/2 \quad (1.3)$$

In the existing literature these equations are usually written in dimen-
sionless variables a and t, by using the unit of length L, and the unit
of time C:

$$L = (3rQW/4\pi\rho gZ)^{1/3} \quad (1.4)$$

$$C = (3/2gZ)^{1/2} L \quad (1.5)$$

Thus $a = A/L$, $t = T/C$, and $\dot{a} = C\dot{A}/L$. Subscripts 0, 1, and 2, refer to
variables at detonation, first maximum, and first minimum.

Since $E_o = rQW = L^3 4\pi P_h/3$, then

$$P_o/(\gamma-1) = P_h a_o^{-3} = P_h k^{-1/(\gamma-1)} \quad (1.6)$$

where k is a convenient notation and is defined by

$$k = a_o^{3(\gamma-1)} = (4\pi\rho gA_o^3 Z/3rQW)^{(\gamma-1)} \quad (1.7)$$

and Eq. 1.3 now reads

$$1.0 - ka^{-3(\gamma-1)} + a_o^3 - a^3 = a^3\dot{a}^2$$

Since $P_o/(\gamma-1) \gg P_h$, that is, $1.0 \gg a_o^3$, the a_o^3 term is usually
dropped and the equation is written:

$$1.0 - ka^{-3(\gamma-1)} - a^3 = a^3\dot{a}^2 \quad (1.8)$$

This approach does not include the effects of fixed and free surfaces,

4

and assumes no migration.

1.2 MIGRATION

During the first half oscillation, the migration is found from experiments to be very small. However, including migration, the kinetic energy term would be[2]

$$KE = 2\pi\rho a^3(\dot{a}^2 + \dot{b}^2/6)$$

Equation 1.8 would now read

$$1.0 - ka^{-3(\gamma-1)} - a^3 = a^3(\dot{a}^2 + \dot{b}^2/6)$$

The migration is usually written[2] in terms of a non-dimensional vertical momentum, s. Since

$$s = a^3\dot{b}/3 \tag{1.9}$$

then the equation of motion, including migration, is

$$1.0 - ka^{-3(\gamma-1)} - a^3 - 3s^2/2a^3 = a^3\dot{a}^2 \tag{1.10}$$

At the maximum and minimum radius, $\dot{a} = 0$. Thus a_1 and a_2 are the largest and smallest roots of

$$1.0 - ka^{-3(\gamma-1)} - a^3 - 3s^2/2a^3 = 0$$

(Note: a_o is also a root of the equation retaining the a_o^3 term since $s_o = 0$.)

The maximum limit of a_1 approaches 1.0 as k (i.e. a_o) and s approach zero. Thus a good approximation to the maximum bubble radius is given by

5

$$a_1 = 1.0 - k/3 - (3\gamma-2)k^2/9 - s_1^2/2 \qquad (1.11)$$

(Reference 2 gives $3s_1^2/2$. This is a typographical error.)

In determining the oscillation period, the momentum term is negligible (as shown by calculations in Appendix 2), and therefore is ignored in all further discussion. Thus, the time to first maximum radius is found from Eq. 1.8 to be:

$$t_1 = \int_{a_0}^{a_1} a^{3/2} (1.0 - a^3 - ka^{-3(\gamma-1)})^{-1/2} \, da \qquad (1.12)$$

Making use of Friedman's I functions (see Appendix 1), $t_1 = I_1$. Assuming $t_2 = 2t_1$, i.e. assuming the integrations from a_0 to a_1 and from a_1 to a_2 are identical, then

$$T_2 = Ct_2 = 2CI_1 \qquad (1.13)$$

1.3 SURFACE EFFECTS

The bubble motion is affected by surfaces, i.e. the bottom, targets, and the air-water interface. Free surfaces repel while fixed surfaces attract the bubble. The oscillation period is reduced by the free surface and increased by the fixed surface. These effects do not cancel; the free surface tends to be stronger. Thus the equation of motion must include surface corrections. The only rigorous surface correction method available is that of Friedman in reference 2 and summarized below. A comparison of Friedman's final equation with those of Kennard[3] is also included.

1.3.1 Friedman's equation

In determining the effect of plane (or spherical) surfaces, the above approach to the equation of motion is valid with one exception. The kinetic energy of the water is found using a velocity potential function which is evaluated using the method of images. This method

is detailed in reference 2. The resulting kinetic energy expression, ignoring second and third order terms and migration, is

$$KE = 2\pi\rho A^3 \dot{A}^2(1.0 + AF/(D+B))$$

where

$$F = 2xf(x) - \ln 2 \tag{1.14}$$

$$x = (d-b)/(d+b) \tag{1.15}$$

$$f(x) = \sum_{n=0}^{\infty} (-1.0)^n \left[(2n+1)^2 - x^2\right]^{-1} \tag{1.16}$$

For tabulated values of x versus F(x), see Appendix 3.

The non-dimensional equation of motion is now

$$1.0 - ka^{-3(\gamma-1)} - a^3 = \left[1.0 + aF/(d+b)\right] a^3 \dot{a}^2 \tag{1.17}$$

Since $\left[1.0 + aF/(d+b)\right]^{1/2} = 1.0 + aF/2(d+b) + \ldots$, then ignoring higher order terms, the time to first maximum radius is

$$t_1 = \int_{a_0}^{a_1} a^{3/2} (1 - a^3 - ka^{-3(\gamma-1)})^{-1/2}(1 + aF/2(d+b))da \tag{1.18}$$

Or in terms of the I functions,

$$t_1 = I_1 + I_2 F/2(d+b).$$

And the oscillation period is

$$T_2 = 2I_1 C \left[1.0 + I_2 LF/2I_1(D+B)\right] \tag{1.19}$$

If the explosive were detonated at a depth such that F = 0 (i.e. at D = 2B), then $T_2 = 2CI_1$. Since this must agree with the well known

7

formula

$$T = KW^{1/3}Z^{-5/6},$$

(1.20)

then the period constant K is defined by

$$K = 2I_1(3/2g)^{1/2}(3rQ/4\pi\rho g)^{1/3}$$

(1.21)

For convenience, a constant is defined:

$$H = I_2(2g/3)^{1/2}/4I_1^2$$

(1.22)

Now Eq. 1.19 reads

$$T = KW^{1/3}Z^{-5/6}\left[1.0 + KW^{1/3}Z^{-1/3}HP/(D+B)\right]$$

(1.23)

This is the form of Friedman's theoretical period formula which will be used later to compute energy partition values (see eq. 2.3).

Next consider the first maximum bubble radius:

$$A_{max} = L(1.0 - k/3 - (3\gamma-2)k^2/9)$$

(1.24)

From Eq. 1.7, k does not equal zero, since A_o cannot be zero. However, in experiments, the error in the measured maximum radius is much greater than the second order correction due to k. Thus A_{max} = L must agree with the well known formula

$$A_{max} = JW^{1/3}Z^{-1/3}$$

(1.25)

This defines the explosive's radius constant J to be

$$J = (3rQ/4\pi\rho g)^{1/3}$$

(1.26)

8

The commonly used K/J ratio is seen to be

$$K/J = 2I_1(3/2g)^{1/2} \tag{1.27}$$

All the I functions depend on k and γ, but from the graphs of $I(k,\gamma)$, in reference 2, $I_1 \geq 0.7405$. Thus,

$$K/J \geq 0.320 \tag{1.28}$$

From the same set of graphs, $I_1^2/I_2 \geq 0.92$, and

$$H \leq 1.26 \tag{1.29}$$

1.3.2 Kennard's equation

Kennard's reports of the early 1940's often give the formula

$$T = KW^{1/3}Z^{-5/6} (1.0 \pm 0.2A_{max}/R)$$

where R is the distance from the charge to the fixed or free surface. The + sign is associated with the attractive force of the fixed (bottom) surface, and the − sign with the repulsive force of the free (air-water) surface. Thus the period would be

$$T = KW^{1/3}Z^{-5/6} (1.0 + 0.2A_{max} (D-B)/DB) \tag{1.30}$$

Usually Eq. 1.30 overcorrects the bottom effect, and also the surface effect in deep shots.

In reference 3, Kennard says 1.30 is an approximate empirical expression and that the theoretical formula, using Friedman's method, is

$$T = KW^{1/3}Z^{-5/6} (1.0 + 0.2P(x)A_{max}(D+B)/DB) \tag{1.31}$$

9

where x is defined by Eq. 1.15 and values of P(x) are calculated from reference 2. Comparing Kennard's graph of P(x) with Friedman's tabulation of F(x), we find

$$P(x) = (1-x^2)F/2 \tag{1.32}$$

Since $A_{max} = La_1$, Eq. 1.31 can be written as

$$T_2 = KW^{1/3}Z^{-5/6}\left[1.0 + 0.4a_1 LF/(D+B)\right] \tag{1.33}$$

This agrees with Friedman's expression (Eq. 1.19) if $I_2/2I_1 = 0.4a_1$. Thus Kennard's eq.1.33 is a special case of Friedman's eq. 1.23.

A choice should be made between Friedman's theoretical period eq. 1.23 involving the complicated F(x) function, and the much simpler eq. 1.30 of Kennard. Friedman's eq. 1.23 is preferred not only because of its theoretical foundation but also because it better fits the experimental data (see page 15).

SECTION 2

ENERGY PARTITION

2.1 ENERGY YIELD OF EXPLOSIVES

Detonation of an explosive releases an amount of energy QW. An
amount $(1-r)QW$ is carried off by the shock wave, leaving the bubble
with rQW for the first oscillation.

Reported values of Q for any one explosive are varied. For example,
for the standard explosive, TNT, they range from around 500 gram calories
per gram weight to over 1000. Keeping in mind that the accuracy of Q
may be improved, Table 2.1 was used in reducing the experimental data
of this report.

TABLE 2.1

Energy Yields

Explosive	Q* (cal/gm)	Q (ft-lb/lb)
TNT	1000	$1.40 \ 10^6$
Pentolite	1220	$1.71 \ 10^6$
RDX + Alum (50/50)	1335	$1.87 \ 10^6$
$2H_2 + O_2$	3794	$5.31 \ 10^6$

Q values are usually reported in calories per gram weight. These
have been converted to the fps system using the conversion factors:

    453.6 grams = 1.0 pound
    1.0 gram calorie = 3.087 foot-pounds

*Private communication: W. W. Perkins, USNRDL.

11

The Q value for $2H_2 + O_2$ is based on the change in enthalpy.

2.2 EVALUATION OF K AND J

The fraction of charge energy left in the bubble for the first oscillation, that is r, can be found using Eqs. 1.21 or 1.26. Thus

$$r = (4\pi\rho g/3Q)K^3(2g/3)^{3/2}/8I_1^3 \qquad (2.1)$$

or

$$r = (4\pi\rho g/3Q)J^3 \qquad (2.2)$$

where I_1 is a function of k and γ, Q is the total charge energy per unit weight, and K and J are constants of the explosive to be determined from experimental data.

In section 1.3, the general form of the equation for the oscillation period was found to be Eq. 1.23. Written as

$$y = K + HK^2 z, \qquad (2.3)$$

where

$$y = Tz^{5/6}W^{-1/3}$$

and

$$z = W^{1/3}Z^{-1/3}F/(D+B),$$

this is the equation for a straight line with slope HK^2 and intercept K. Using the method of least squares (Appendix 5) to fit the explosive's experimental data (for varying charge depth, pond depth, and perhaps charge weight), the values of K and H can be computed for the explosive.

Using a least squares fit, it is possible to minimize the error in y or in z. From the experimental data of Appendix 4, the first order variable y is at least a factor of 100 times the second order variable z. Therefore the following values of K and H were computed based on minimizing the error in y.

12

TABLE 2.2

First and Second Order Period Constants

Explosive	K	K'	H
Pentolite	4.59	4.30	1.23
RDX + Alum (50/50)	4.89	4.44	1.32
$2H_2O + O_2$	6.50	4.17	1.50

This needs some explanation. The K values are based on actual charge weight (except for RDX + Alum where 0.8 pounds was used; that is, the Alum weight was excluded). However if, instead of the actual weight, the equivalent weight TNT (i.e. QW/Q_{TNT}) is used, the K' values compare with those found in the literature which vary from 4.19 to 4.37 for TNT and Pentolite.

From Eq. 1.29, the largest possible value of H is 1.26. Thus except for Pentolite the above H values are too high, but these high values can be explained by experimental error (see Appendix 6). If the error in z were minimized, the H values would be still higher.

J can be determined from Eq. 1.27 if the value of I_1 (k,γ) is known. The ratio of specific heats of the bubble's gas is not always known, but it is standard procedure to let

$$\gamma = 1.25 \tag{2.4}$$

Thus to determine J, k must be evaluated. But from Eq. 1.7, k is a function of the energy partition r.

2.3 ENERGY PARTITION VALUES

As shown in section 2.2, the energy partition can be determined from Eq. 2.1 by a trial and error method since $r = f(I_1) = f(k) = f(r)$. In other words, it is a circular relationship. To simplify things, we solve for $k(I_1)$ by eliminating r between Eqs. 1.7 and 1.21. Thus

$$k = \left[(Z/W)(3/2g)^{3/2}(2I_1A_0/K)^3 \right]^{(\gamma-1)} \tag{2.5}$$

From the experiments, the charge radii in feet are: Pentolite, 0.1354; RDX + Alum (50/50), 0.1458; $2H_2 + O_2$, 0.50. Equation 2.5 gives one relationship between k and I_1. From reference 2, the graph of I_1 versus k for $\gamma = 1.25$ gives a second relationship. The intersection of the two curves gives the sought for values of k and I_1. J is found from K and I_1. Knowing k yields I_1^2/I_2, and thus H from Eq. 1.22. Finally, r is found from Eq. 2.1. The results are below.

TABLE 2.3.1

Energy Partition Values ($\gamma = 5/4$)

Explosive	k	I_1	J	J'	H	r
Pentolite	0.075 ± .001	.7423	14.32	13.42	1.23	0.45
RDX + Alum	0.081 ± .001	.7420	15.26	13.86	1.23	0.50
$2H_2 + O_2$	0.213 ± .008	.7410	20.32	13.03	1.14	0.41

where the ± values are due to the depth (Z) variation.

For sea water, i.e. $\rho g = 64$ lb/ft^3, the respective r values are 0.46, 0.51 and 0.42.

The effect of increasing γ from 5/4 to 4/3 is shown below.

TABLE 2.3.2

Energy Partition Values ($\gamma = 4/3$)

Explosive	$k = a_0$	I_1	J	J'	H	r
Pentolite	0.032 ± .001	.7480	14.21	13.31	1.24	0.44
RDX + Alum	0.035 ± .001	.7482	15.14	13.74	1.24	0.49
$2H_2 + O_2$	0.127 ± .006	.7550	19.94	12.79	1.17	0.39

Again, for sea water, the respective r values are .45, .50, .40.

14

The ratio of internal energies at maximum radius and initial radius is $E_1/E_0 = (a_0/a_1)^{3(\gamma-1)}$. For $\gamma = 5/4$, these ratios are 0.077, 0.083, and 0.227 for Pentolite, RDX + Alum (50/50), and $2H_2 + O_2$. For $\gamma = 4/3$, the ratios decrease to 0.032, 0.035, and 0.113.

All of the above calculations are based on Friedman's method. If we use a least squares fit of the experimental data to Kennard's eq. 1.30, we find the intercept K and slope KJa_1 of the straight line. Using the calculated K values, and assuming $I_1 = 0.741$, the respective energy partition values are 0.38, 0.41, and 0.33. Using the calculated KJa_1 values, and assuming $a_1 = 1.0$, the respective energy partition values are 0.49, 0.67, and 0.83. (Assuming a_1 is some value less than 1.0 would increase this second set.)

If Kennard's eq. 1.30 were a better fit of the experimental data than Friedman's eq. 1.23, then the two sets of data should agree. Since they differ radically, Friedman's eq. 1.23 is a better fit.

CONCLUSIONS

The theoretical equation for the bubble oscillation period, including the effects of surfaces, was found to be Friedman's:

$$T_2 = KW^{1/3}Z^{-5/6}(1.0 + KW^{1/3}Z^{-1/3}HF/(D+B))$$

Using the method of least squares to fit the experimental periods of three selected explosives, the period constants K were determined. The error in K was calculated to be less than 5.5% based on maximum probable variations in the experimental variables. The energy partition values of the explosives were then found using the method discussed in Section 2.3. This involved assuming that γ, the ratio of specific heats of the bubble gas, was 1.25. The resulting r values for Pentolite, RDX + Alum, and $2H_2 + O_2$, were 0.45, 0.50, and 0.41, respectively.

Increasing γ would decrease the resulting energy partition values. For example, for $2H_2 + O_2$, if γ is increased from 1.25 to 1.50, r is decreased from 0.41 to 0.38.

From Eq. 2.1, the accuracy of r is directly proportional to the accuracy of Q (probably $\pm$ 10% at best) and to the cube of K's accuracy ($\pm$ 17%). Thus the minimum probable experimental accuracy for r is $\pm$ 27%, and the energy partition values, including error variation, are 0.45 ± 0.12, 0.50 ± 0.14, and 0.41 ± 0.11, respectively. Although the best available experimental data was used, the minimum probable error variation in r is greater than the variation due to type of explosive.

There is a tendency for the steam bubble to retain slightly less energy than non-condensable gas bubbles for the bubble oscillation. But, based on energy partition considerations, it makes little difference which explosive is selected to simulate the nuclear case.

16

APPENDIX 1

THE I FUNCTIONS

The I functions are used in determining the oscillation period (I_1 and I_2), the vertical momentum (I_3, I_4, I_5, and I_6), and the vertical displacement of the bubble (I_7 and I_8). They are:

$$I_1 = \int_{a_0}^{a_1} u^{-1} a^{3/2} \, da$$

$$I_2 = \int_{a_0}^{a_1} u^{-1} a^{5/2} \, da$$

$$I_3 = \int_{a_0}^{a_1} u \, a^{5/2} \, da$$

$$I_4 = \int_{a_0}^{a_1} u \, a^{7/2} \, da$$

$$I_5 = \int_{a_0}^{a_1} u^{-1} a^{9/2} \, da$$

$$I_6 = \int_{a_0}^{a_1} u^{-1} a^{11/2} \, da$$

$$I_7 = \int_{a_2}^{a_1} (u^2 - 3s^2/2a^3)^{-1/2} a^{-3/2} \, da$$

$$I_8 = \int_{a_2}^{a_1} (u^2 - 3s^2/2a^3)^{-1/2} a^{-1/2} \, da$$

where $u = (1 - a^3 - ka^{-3(\gamma-1)})^{1/2}$.

Graphs of the first six I functions for $\gamma = 1.25$, 1.33, 1.40, 1.50,

and $0 \leq k \leq 0.3$, are given in reference 2. A check on their limit values (at $k = 0$), using the beta function

$$\beta(m,n) = \int_0^{1.0} v^{m-1} (1-v)^{n-1} \, dv \quad \text{for } m > 0, \ n > 0,$$

where $v = a^3$, agrees with the graphs and gives: $I_1 = 0.7468$, $I_2 = 0.6072$, $I_3 = 0.1821$, $I_4 = 0.1309$, $I_5 = 0.4668$, $I_6 = 0.4250$, and $I_1^2 / I_2 = 0.9186$. Except for I_1 and I_1^2 / I_2, these are all upper limit values.

This method cannot be used to determine the limit values of I_7 and I_8 since they are integrated from a_2 to a_1, and a_2 is not zero. Evaluation of I_7 and I_8, using numerical integration, is possible but very involved because of the s^2 term (see Appendix 2).

VERTICAL MOMENTUM

The vertical momentum of the bubble at its maximum radius, $s_1 = a_1^3 \dot{b}_1/3$, is reported in reference 2 to be:

$$s_1 = (L/Z)\left[I_5 + LFI_6/2(D+B)\right] - 2L^2\dot{F}/(D+B)^2\left[I_3 - LFI_4/2(D+B)\right]$$

where $\dot{F} = dF/dx$. The first term is the upward momentum due to gravity, and the second term is the downward momentum due to the rigid surface. The vertical momentum at the bubble minimum is twice this value.

Usually the migration at maximum radius is considered negligible. However, to determine the effect of s_1 in Eq. 1.11, the calculations in Table A.2 were made.

TABLE A.2

Vertical Momentum

Explosive	D = 4.05 ft			D = 9.0 ft		
	s_1	$s_1^2/2$	a_1	s_1	$s_1^2/2$	a_1
Pentolite	-.0750	+.0028	0.9711	+.0064	+.00002	0.9739
RDX + Alum	-.0696	+.0024	0.9693	+.0072	+.00003	0.9717
$2H_2 + O_2$	-.0200	+.0002	0.9200	+.0120	+.00007	0.9202

Increasing depth increases s_1. Since s_1 is less than zero at shallow depth, $s_1^2/2$ decreases to a negligible value at mid-depth.

APPENDIX 3

Table A.3

Friedman's Surface Correction Function: $F(x)$

x	$F(x)$	x	$F(x)$
0	− 0.693		
− .05	− 0.785	+ .05	− 0.601
− .10	− 0.878	.10	− 0.508
− .15	− 0.975	.15	− 0.412
− .20	− 1.076	.20	− 0.310
− .25	− 1.184	.25	− 0.202
− .30	− 1.307	.30	− 0.085
− .35	− 1.431	.35	− 0.045
− .40	− 1.577	.40	0.191
− .45	− 1.744	.45	0.358
− .50	− 1.939	.50	0.553
− .55	− 2.174	.55	0.788
− .60	− 2.462	.60	1.076
− .65	− 2.829	.65	1.443
− .70	− 3.312	.70	1.926
− .75	− 3.985	.75	2.599
− .80	− 4.991	.80	3.605
− .85	− 6.661	.85	5.275
− .90	− 9.998	.90	8.612
− .95	−20.000	.95	18.620
−1.00	− ∞	1.00	∞

The following series expression was found to agree with the above tabulation:

$$F = -0.693 + 1.832x + 1.978x^3 + 2x^5(1-x^2)^{-1}$$

APPENDIX 4

EXPERIMENTAL DATA

Three explosives were studied in the Hydra test pond during the summer of 1960. They were: Pentolite, the control; an equal mixture by weight of RDX + Alum (Al $NH_4(SO_4)_2 \cdot 12H_2O$); and a pressurized stoichiometric mixture of hydrogen and oxygen in a frangible plastic sphere. All charges were spherical and centrally detonated. They were detonated at various depths in the hemispherical pond of 18-ft radius. Bubble radii and periods were measured[*].

MAXIMUM BUBBLE RADIUS

A high speed Photosonic camera was mounted underwater, about 25 ft from the charge (in a camera bay). A six inch wire grid was mounted midway between the camera and the charge. Films showing a well defined first oscillation were reduced using the grid lines, for the first maximum horizontal diameter. The experimental J values ($J_{exp} = AZ^{1/3}W^{-1/3}$) are compared with the theoretical $J'a_1$ values in Table A.4.1.

TABLE A.4.1

Radius Constants

Explosive	J_{exp}	$J'a_1$
Pentolite	12.96 ± 0.48	13.07
RDX + Alum	13.01 ± 0.24	13.47
$2H_2 + O_2$	11.99 ± 0.54	11.97

[*] Complete experimental details can be obtained from W.W. Perkins

21

BUBBLE PERIOD

Bubble periods were measured by recording on an oscilliscope camera, the pressure signal from a tourmaline piexoelectric gauge set about 12 ft from the charge. Initially the scope swept twenty milliseconds per centimeter, recording the time between the shock wave and the bubble pulse. Later in the series, in order to more accurately determine the depth effect on the period, the scope was delayed a set time (150 to 180 msec) from the initiating pulse and then swept slower (from 0.5 to 5.0 msec/cm) to record the bubble pulse only. In some cases the estimated delay time was incorrect and the bubble pulse was partially or entirely missed. But where the period was obtained, it was at least four times more accurate than those from the earlier method.

The following tabulated data are periods obtained using the delay method. Since the same pulse triggered both the explosive and the scope delay circuit, the observed time on the oscilliscope included the time of arrival of the first minimum pressure pulse. This arrival time was found to be 2.4 msec for Pentolite and RDX + Alum (50/50), and 2.8 msec for $2H_2 + O_2$. The periods in Tables A.4.2 - A.4.4 have been corrected.

TABLE A.4.2

Experimental Pentolite Periods

WEIGHT: 1.06 lb

GAUGE: 0.5 inch diameter, except where noted

DETONATOR: Engineer's Special (0.875 g PETN, plus mercury fulminate)

Shot	D (ft)	D+B (ft)	T_{exp} (sec)	T_{calc} (sec)	ΔT (sec)
66	4.3	18	.1906	.1850	-.0056
67	4.3	18	.1896	.1850	-.0046
67	4.3	18	.1896	.1850	-.0046
50	5.0	18	.1866	.1892	+.0026
51	5.0	18	.1875	.1892	+.0017
901	5.0	18	.1859	.1892	+.0033
901*	5.0	18	.1854	.1892	+.0038
902	5.0	18	.1851	.1892	+.0041
902*	5.0	18	.1842	.1892	+.0050
75	7.0	19	.1956	.1936	-.0020
74	9.5	19	.1966	.1937	-.0029

*1.0 inch diameter gauge.

TABLE A.4.3

Experimental RDX + Alum (50/50) Periods

WEIGHT: 0.8 lb of RDX, plus 0.8 lb of Alum

GAUGE: 0.5 inch diameter, except where noted

DETONATOR: Modified Engineer's Special (0.875 grams tetryl, plus lead azide, plus a 2.5 gram tetryl booster)

Shot	D (ft)	D+B (ft)	T_{exp} (sec)	T_{calc} (sec)	ΔT (sec)
90*	4.0	18	.1746	.1749	+.0003
96*	4.0	18	.1770	.1749	-.0021
96	4.0	18	.1772	.1749	-.0023
94*	5.0	18	.1792	.1818	+.0026
94	5.0	18	.1804	.1818	+.0016
93*	6.0	18	.1826	.1854	+.0028
56	9.5	19	.1882	.1871	-.0011
57	9.5	19	.1886	.1871	-.0015

*1.0 inch diameter gauge.

TABLE A.4.4

Experimental $2H_2 + O_2$ Periods

GAUGE: 0.5 inch diameter, except where noted

DETONATOR: Pyrofuze (Palladium and Aluminum alloy wire)

Shot	W (lb)	D (ft)	D+B (ft)	T_{exp} (sec)	T_{calc} (sec)	ΔT (sec)
62	0.3175	4.0	19	.1712	.1649	-.0063
70	0.2635	4.0	18	.1572	.1581	+.0009
77	0.2635	6.0	19	.1582	.1683	+.0101
87*	0.2635	6.0	18	.1672	.1686	+.0014
92*	0.2635	6.0	18	.1678	.1686	+.0008
92	0.2635	6.0	18	.1687	.1686	-.0001
76	0.2635	8.0	19	.1732	.1707	-.0025
61	0.3175	9.5	19	.1862	.1812	-.0050

*1.0 inch diameter gauge.

APPENDIX 5

METHOD OF LEAST SQUARES

The best linear fit to a series of values is a line about which the sum of the squares of the deviations is a minimum. Applying this principal to $y = K + HK^2 z$, and minimizing the error in y, we find:

$$K = (\Sigma y \Sigma z^2 - \Sigma z \Sigma yz)/(N \Sigma z^2 - \Sigma z \Sigma z)$$

$$HK^2 = (\Sigma y \Sigma z - N \Sigma yz)/(\Sigma z \Sigma z - N \Sigma z^2)$$

where N is the number of data sets (y, z).

If the error in z were minimized, then:

$$K = (\Sigma y \Sigma yz - \Sigma z \Sigma y^2)/(N \Sigma yz - \Sigma y \Sigma z)$$

$$HK^2 = (\Sigma y \Sigma y - N \Sigma y^2)/(\Sigma y \Sigma z - N \Sigma yz)$$

APPENDIX 6

ERRORS IN K AND H

From the method of least squares, K is proportional to y which equals $TZ^{5/6}W^{-1/3}$, and H is proportional to $1/yz$ which equals $(D+B)/TFZ^{1/2}$. Thus any errors in the measurement of the period and or the depths will affect the accuracy of K and H. K will also be affected by weight errors. From the experimental data, the period errors and the weight errors are each less than 2%. To determine the effect of the depth error, the following assumptions were made: (1) the error in charge depth D due to water sur- face wave motion is less than 0.18 feet, and (2) the pond depth error, due to water blown out by preceding shots, is less than 0.5 feet.

Then for this data, the 0.5 foot variation in pond depth will cause less than 4.7% error in $(D+B)/F$. The 0.18 foot variation in charge depth will cause less than 0.4% error in $Z^{5/6}$ and less than 5.6% error in $FZ^{1/2}$. The hydrostatic charge depth in sea water is D+33 feet while in fresh water it is D+34 feet. The variation is less than 2.3% in $Z^{5/6}$ and less than 1.4% in $Z^{1/2}$.

Thus, from the above assumptions, the total error in K is less than 5.5% and the total error in H is less than 14%.

An additional possible error in the experimentally determined K should be mentioned here. Rudlin's work[*] indicates that for spherical explosives, the fraction of the charge consumed is a function of the

---

* L. Rudlin. An Approximate Solution of the Flow Within the Reaction Zone Behind a Spherical Detonation Wave in TNT. U.S. Naval Ordnance Laboratory. NAVWEPS 7364, April 1961.

charge size. Assuming Rudlin's theory for TNT applies for Pentolite, the following values were calculated. Here N is the fraction of explosive consumed.

W(lbs)	N
0.05	0.759
1.06	0.880
416.00	0.942

The experimental value of K' was found to be 4.30 for a 1.06 pound Pentolite charge. But if only 88% of the explosive was consumed, the actual weight was .88 x 1.06 pounds. Since $KW^{1/3}$ is constant, the experimentally determined K' value can be predicted to vary with the charge weight: $K'_{exp} = 4.49 \ N^{1/3}$. In other words, the K' value found with a 1.06 pound Pentolite charge should be 2% less than the K' value found using a 416 pound charge and 5% higher than the K' value found using a 0.05 pound charge. This effect should not apply to the $2H_2 + O_2$ explosive.

SYMBOLS

All dimensions are in the fps system

A	bubble radius
a	non-dimensional radius
B	charge distance from bottom
b	B/L
C	unit of time
D	charge depth
d	D/L
E	internal bubble energy
F, F(x)	function giving surface effects on period
f(x)	function giving surface effects on period
g	acceleration of gravity
H	second order bubble period constant
I	see Appendix I
J	bubble radius constant
K	bubble period constant
KE	kinetic energy of water
k	$a_o{}^{3(\gamma-1)}$

L	unit of length
P	bubble pressure
P_h	hydrostatic pressure at charge depth; $= \rho g Z$
Q	charge energy per unit weight
r	fraction of charge energy in bubble
s	non-dimensional vertical momentum of bubble
T	time variable
T_2	time to first minimum, i.e. bubble period
t	non-dimensional time variable; $= T/C$
V	bubble volume
W	charge weight
WD	work of displacement
x	(D-B)/(D+B)
Z	D+33 ft (34 for fresh water)
γ	ratio of specific heats of bubble gas
ρ	mass density of water

REFERENCES

1.   C. Ramsauer. Die Massenbewegung des Wassers bei Unterwasser
Explosionen (Mass Movement of Water in Underwater Explosions). Annalen
der Physik 72:265-284, 1923

2.   B. Friedman. Theory of Underwater Explosion Bubbles. Institute
for Mathematics and Mechanics, New York University, September 1947.
(Also, Underwater Explosion Research. Vol II The Gas Globe. Office
of Naval Research, Department of the Navy, 1950)

3.   E.H. Kennard. Underwater Explosions - A Summary of Results.
David Taylor Model Basin C-334, p 54, February 1951 (Confidential).

INITIAL DISTRIBUTION

NO.
CPY

NAVY

1	CHIEF, BUREAU OF SHIPS (CODE 320)
3	CHIEF, BUREAU OF SHIPS (CODE 210L)
1	CHIEF, BUREAU OF SHIPS (CODE 362B)
1	CHIEF, BUREAU OF SHIPS (CODE 423)
1	CHIEF, BUREAU OF NAVAL WEAPONS (RRMA-11)
1	CHIEF, BUREAU OF NAVAL WEAPONS (RRE-5)
2	CHIEF, BUREAU OF YARDS AND DOCKS (CODE 42.330)
1	CHIEF, BUREAU OF YARDS AND DOCKS (CODE 50)
1	DIR. BUREAU OF YARDS —DOCKS(NORTHWEST DIV)
1	CHIEF OF NAVAL OPERATIONS (OP-07T)
1	CHIEF OF NAVAL OPERATIONS (OP-446)
1	OFFICE OF THE CHIEF OF NAVAL OPERATIONS (OP-75)
1	CHIEF OF NAVAL RESEARCH (CODE 104)
1	DIRECTOR, NAVAL RESEARCH LABORATORY (CODE 2021)
1	CHIEF OF NAVAL RESEARCH (CODE 418)
5	CO. OFFICE OF NAVAL RESEARCH, FPO, NEW YORK
1	CO.,-US NAVAL CIVIL ENGINEERING LABORATORY
1	CO, NAVAL AIR DEVELOPMENT CENTER
1	COMM. U.S. NAVAL ORDNANCE LAB., WHITE OAK (CODE EU)
1	COMM. U.S. NAVAL ORDNANCE LAB., WHITE OAK (CODE E)
1	COMM. U.S. NAVAL ORDNANCE LAB., WHITE OAK (CODE EA)
1	CDR NAVAL ORDNANCE TEST STATION
1	CO, U.S. NAVY ORDNANCE TEST STATION, PASADENA
1	DIRECTOR, NAVAL WEAPONS LABORATORY,DAHLGREN
1	CO, U.S. NAVAL WEAPONS LAB.
1	CO-DIR. NAVY ELECTRONICS LAB. (CODE 2632C)
1	CO-DIR. NAVY ELECTRONICS LAB. (CODE 2350)
1	CO-DIR, DAVID TAYLOR MODEL BASIN (CODE 775)
1	CO-DIR, DAVID TAYLOR MODEL BASIN (CODE 700)
1	CO, DAVID W TAYLOR MODEL BASIN (UERD, CODE 780)
1	COMM. WESTERN SEA FRONTIER
1	DEP. COMM., OPERATIONAL TEST —EVALUATION FORCE, PAC.
1	COMM. OPERATIONAL TEST-EVALUATION FORCE, ATLANTIC
1	DIRECTOR, ARMED FORCES RADIOBIOLOGY RESEARCH INSTITUTE

ARMY

1	OFFICE OF CHIEF RESEARCH AND DEVELOPMENT (ATOMIC OFFICE)
1	CHIEF OF RESEARCH AND DEVELOPMENT (LIFE SCIENCE DIV)
1	DEPUTY CHIEF OF STAFF FOR MILITARY OPERATIONS (CBR)
1	CHIEF OF ENGINEERS (ENGMC-EB)
1	CHIEF OF ENGINEERS (ENGMC-DE)
1	OFFICE OF CHIEF OF ENGINEERS (ENGCW-Z)
1	CG ARMY MATERIEL COMMAND (AMCRD-DE-NE)
1	CG, BALLISTIC RESEARCH LABORATORIES
1	U S ARMY EDGEWOOD ARSENAL

```
1     CO U.S.ARMY CBR COMBAT DEV COMMAND FT. MCCLELLAN)
1     COMMANDANT, CHEMICAL CORPS SCHOOLS (LIBRARY)
1     CO, CHEMICAL RESEARCH AND DEVELOPMENT LABORATORIES
1     COMMANDER, NUCLEAR DEFENSE LABORATORY
1     COMMANDANT ARMY WAR COLLEGE
1     DIRECTOR, WALTER REED ARMY INSTITUTE OF RESEARCH
1     CG, COMBAT DEVELOPMENTS COMMAND (CDCMR-V)
1     CG, QUARTERMASTER RES AND ENG COMMAND
1     HQ, DUGWAY PROVING GROUND
3     THE SURGEON GENERAL (MEDPS-NM)
1     DIRECTOR, USACDS NUCLEAR GROUP
1     DIRECTOR, WATERWAYS EXPERIMENT STATION
1     CG, MUNITIONS COMMAND  (PICATINNY ARSENAL)
2     CO, WATERTOWN ARSENAL
1     CG, ARMY MISSILE COMMAND (REDSTONE ARSENAL)


      AIR FORCE


1     ASSISTANT CHIEF OF STAFF  INTELLIGENCE (AFCIN-3B)
5     CG, AERONAUTICAL SYSTEMS DIVISION (ASAPRD-NS)
1     DIRECTORATE OF CIVIL ENGINEERING (AFOCE-ES)
1     DIR. THE RAND CORP. (DR. RAPP)
1     COMMANDANT, SCHOOL OF AEROSPACE MEDICINE, BROOKS AFB
1     OFFICE OF THE SURGEON (SUP3.1), STRATEGIC AIR COMMAND
1     CG SPECIAL WEAPONS CENTER  KIRTLAND AFB
1     DIRECTOR, AIR UNIVERSITY LIBRARY, MAXWELL AFB
2     COMMANDER, TECHNICAL TRAINING WING, 3415TH TTG
1     COMMANDER, AIR FORCE CAMBRIDGE RSCH LABS.(CRT)
1     HQ, AIR FORCE TECHNICAL APPLICATIONS CENTER


      OTHER DOD ACTIVITIES


3     CHIEF, DEFENSE ATOMIC SUPPORT AGENCY (DASARA-3)
3     CHIEF, DEFENSE ATOMIC SUPPORT AGENCY (LIBRARY)
1     COMMANDER,FC/DASA, SANDIA BASE (FCDV)
1     COMMANDER, FC/DASA, SANDIA BASE (FCTG5, LIBRARY)
1     COMMANDER, FC/DASA, SANDIA BASE (FCWT)
2     OFFICE OF CIVIL DEFENSE (DIR OF RSCH)
2     OFFICE OF CIVIL DEFENSE, WASHINGTON
2     CIVIL DEFENSE UNIT, ARMY LIBRARY
3     DIRECTOR ADVANCE RESEARCH PROJECTS AGENCY
20    DEFENSE DOCUMENTATION CENTER


      AEC ACTIVITIES AND OTHERS


1     ATOMIC ENERGY COMMISSION (DR. HOOPER)
1     ATOMIC ENERGY COMMISSION (DR. JOSEPH)
1     U.S. ATOMIC ENERGY COMMISSION (HOLLISTER)
1     CALIFORNIA INSTITUTE OF TECHNOLOGY
1     HARVEY MUDD COLLEGE
1     DIR. HAWAII MARINE LAB.
1     LAMONT GEOPHYSICAL LABORATORY
1     LOS ALAMOS SCIENTIFIC LABORATORY (LIBRARY)
1     MICHIGAN STATE UNIVERSITY (TRIFFETT)
1     RESEARCH ANALYSIS CORPORATION
```

34

1	PRESIDENT, SANDIA CORP. (DR. REED)
1	PRESIDENT, SANDIA CORP. (MERRITT)
1	DIR. SCRIPPS INST. OF OCEANOGRAPHY (VAN DORN)
1	DIR. SCRIPPS INST. OF OCEANOGRAPHY (DR. FOLSOM)
1	ST. OF CALIF. DEPT. OF FISH AND GAME (BISSEL)
2	U. OF CALIFORNIA LAWRENCE RADIATION LAB, LIVERMORE
1	U. OF CALIF. LAWRENCE RADIATION LAB. (DR. SHELTON)
1	UNIVERSITY OF HAWAII (DR.COX)
1	UNIVERSITY OF WASHINGTON (DONALDSON)
1	US COAST AND GEODETIC SURVEY, SAN FRANCISCO
3	US COAST AND GEODETIC SURVEY, WASHINGTON
1	US GEOLOGICAL SURVEY, DENVER
1	US GEOLOGICAL SURVEY, MENLO PARK
1	US GEOLOGICAL SURVEY, NAVAL WEAPONS PLANT
1	US GEOLOGICAL SURVEY, WASHINGTON
1	WOODS HOLE OCEANOGRAPHIC INSTITUTE

USNRDL

50	TECHNICAL INFORMATION DIVISION

DISTRIBUTION DATE: 6 January 1964

35

Naval Radiological Defense Laboratory
USNRDL-TR-702
HYDRA PROGRAM - THEORETICAL AND EXPERIMENTAL DETERMINATION OF ENERGY PARTITION OF SELECTED UNDERWATER EXPLOSIVES by M. Kaltwasser 28 October 1963 38 p. tables 3 refs.
UNCLASSIFIED

A summary is presented of the derivation of the equation of motion of the bubble due to an underwater spherical explosion. Migration and surface effects are included. The formulae for the first maximum radius and the first oscillation period,
(over)

1. Explosion bubbles - Test methods.
2. Underwater explosions - Simulation.
3. Explosive materials.
I. Kaltwasser, M.
II. Title.

UNCLASSIFIED

including surface effects, are given.
From the experimentally determined bubble period data and the theoretical period formula:

$$T_2 = KW^{1/3}Z^{-5/6}\left[1.0 + KW^{1/3}Z^{-1/3}H_F/(D+F)\right]$$

the energy partition of three explosives, Pentolite, RDX + Alum (50/50), and $2H_2 + O_2$ are calculated.

UNCLASSIFIED